CALCULATION OF TIME CONSTANTS FOR INTRACELLULAR DIFFUSION IN WHOLE CELL PATCH CLAMP CONFIGURATION

CARLOS OLIVA, IRA S. COHEN, AND RICHARD T. MATHIAS
Department of Physiology and Biophysics, State University of New York at Stony Brook, Stony Brook, New York 11794-8661

ABSTRACT We present a simplified model to identify and analyze the important variables governing the diffusion of substances from pipettes into canine cardiac Purkinje cells in the whole cell patch clamp configuration. We show that diffusion of substances through the pipette is the major barrier for equilibration of the pipette and cellular contents. We solve numerically the one-dimensional diffusion equation for different pipette geometries, and we derive a simple analytic equation which allows one to estimate the time necessary to reach the steady state of intracellular concentration. The time constant of the transient to steady state is given by a pipette geometric factor times the cell volume divided by the diffusion coefficient of the substance of interest. The geometric factor is shown to be given by the ratio of pipette resistance to the resistivity of the filling solution. Additionally, from our modeling, we concluded that pipette perfusion at distances >20 μm from the pipette tip would not substantially reduce the time necessary to achieve the steady state.

INTRODUCTION

Development of the gigaohm seal patch clamp technique has allowed voltage clamp investigation of many cell types that had previously not been studied (1). A major advantage of this technique is that substances placed in the pipette will diffuse into the cell allowing the experimenter some control of the intracellular environment. In this manner, the roles of a variety of second messengers have been examined (2, 3). In a modification of this technique, pipettes with perfusion have been developed that allow the exchange of pipette contents at some fixed distance, 100–300 μm from the pipette tip (4). This technical advance has allowed the use of a number of intracellular solutions on a single cell, and has been used successfully to study the ionic dependence of Na^+/Ca^{+2} exchange (5) and voltage dependence of the Na^+/K^+ pump (6).

We became concerned about the speed with which pipette contents exchange with the intracellular milieu during experiments designed to reduce intracellular $[K^+]$ to one-sixth normal in isolated Purkinje myocytes from the canine heart. In these roughly cylindrical cells of 180 μm in length and 30 μm in diameter, it could take >30 min for the exchange to reach steady state (Cohen, I. S., D. DiFrancesco, N. K. Mulrine, and P. Pennefather, submitted for publication). In investigating the literature for an explanation of this slow pipette-cell exchange, we discovered two attempts to quantitatively model this question. Kameyama et al. (2) examined the diffusion of cAMP into a ventricular cell by numerically solving the diffusion equations. The difficulty in applying their result to our problem was that no general conclusions concerning the relationship between the relevant variables (pipette geometry, cell volume, diffusion coefficient) and the time to steady state were provided. In quite a different approach, Mogul et al. (7) solved diffusion in three dimensions within a ventricular cell and included membrane transport, however their boundary conditions ignored the importance of the pipette in determining the time course of exchange. This later approach to model the diffusion of substances from pipette to cell does not provide a slow enough pipette-cell exchange to account for our observations. We felt that diffusion in the pipette might be the rate limiting factor of pipette-cell exchange, and, with this idea in mind, we modeled the diffusion of substances from pipette to cell.

GLOSSARY

a (cm)	Distance on the x axis between the perfusion point at $x = 0$ and the pipette tip (see Fig. 1)
b (cm)	Distance on the x axis between the perfusion point at $x = 0$ and the cell membrane opposite to the pipette tip (see Fig. 1)
d (cm)	Distance on the x axis between the perfusion point at $x = 0$ and the apex of the projection into the cell of the conical shank
r (cm)	Radius. With the subscript p, it refers to pipette tip radius
s (s^{-1})	Variable in the exponential of the Laplace Trans-

Address correspondence to Carlos Oliva.

	form. See first integral equation of Section 2 in Appendix I
A (cm^2)	Cross-sectional area
$C(x, t)$ (mol/cm^3)	Concentration at distance x and time t
D (cm^2/s)	Diffusion coefficient
L (cm)	Cell length
R (Ω)	Electrical resistance of pipette shank
V (cm^3)	Cell volume
α (degrees)	Semi-cone angle of conical pipette shank
ρ (Ω-cm)	Resistivity of pipette filling solution

Subscripts

p Refers to pipette
c Refers to cell

Superscripts

\+ On the right hand side of
– On the left hand side of

THEORY AND METHODS

Assumptions

In the whole cell patch clamp configuration, substances diffuse from the pipette electrode into the cell. We studied the variables affecting the time necessary to achieve a steady state of intracellular concentration. To study this diffusion process, we made a number of simplifying assumptions.

(*a*) Particles move only by diffusion. No external forces act on the diffusing particles. This means, we did not include in our calculations any electric forces or flow of fluid driven by pressure gradients.

(*b*) Diffusion is in one dimension. We assumed that intracellular diffusion is instantaneous in directions perpendicular to the x axis, but the x directed flux is scaled appropriately when the cross-sectional area changes (see Fig. 1 for a description of the placement of the coordinate axes in our calculations).

(*c*) The cell membrane is impermeable to the diffusing particles. No transport or leak of the diffusing particles is assumed to occur through the cell membrane. The steady-state intracellular concentration may differ from the concentration at the perfusion plane if there is transport or leak of the diffusing particles through the cell membrane.

(*d*) Pipette perfusion is modeled as an infinite planar source of diffusing particles. Perfusion of the pipette is experimentally accomplished by inserting a small capillary into the electrode where the fluid is quickly exchanged by convection (4). We assumed that the major effect of this quick exchange of fluid is to keep the concentration constant at the plane of perfusion.

(*e*) We modeled the shank of the pipette as being either cylindrical or conical.

(*f*) Cells are assumed to be rectangular parallelepipeds. Our calculations were directed to study the diffusion of particles from pipette electrodes into canine cardiac Purkinje cells which have a somewhat cylindrical shape. The radius of the cells is ~15 μm, and the length ~180 μm. Because we were not concerned with the details of intracellular diffusion, we modeled the cells as rectangular parallelepipeds of 30 μm in width, 30 μm in height, and 180 μm in length.

Methods

To solve the problem, we Laplace transformed the diffusion equations, and we derived the Laplace transform of the intracellular concentration. We also derived an analytic expression for the average transformed intracellular concentration by integrating from one end of the cell to the other. Using an IMSL subroutine on an IBM PC, we inverted numerically the Laplace transforms to obtain the time course of the spatial distribution of concentration and the time course of the average intracellular concentration change. In Appendix I, we present the analytic expressions for the transformed concentrations.

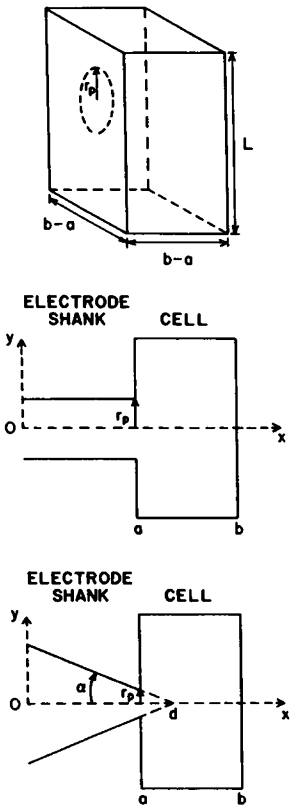

FIGURE 1 A cross-section of the pipette shank and cell. The cell is assumed to be a rectangular parallelepiped of volume $A_c(b - a)$, whereas the pipette is cylindrical in the upper panel and conical in the lower. The coordinates, distances, and geometrical parameters are defined by the sketches. Note that the distance d represents a mathematical point in the cell that is projected by the semi-cone angle, α, of the shank.

RESULTS

In our calculations, the length of the cell, L, was 180 μm, the cell cross-sectional area, A_c, was 30 × 180 μm, and its width, $(b - a)$, was 30 μm. The diffusion constant of the diffusing particles, D, was 10^{-5} cm^2/s. The resistivity of the pipette filling solution was 100 Ω-cm.

1. Concentration Profiles

Fig. 2 shows the evolution of concentration profiles in the pipette shank and in the cell, for conical and cylindrical pipette shanks. The intracellular concentration profiles are much flatter than the pipette's concentration profiles. The general shapes of the concentration profiles we calculated are similar to the ones calculated by Kameyama et al. (2). They modeled the diffusion of particles from conical pipette shanks into guinea pig ventricular cells, and they employed a different numerical method. This result suggests that the average intracellular concentration is an accurate measure of the concentration anywhere in the cell and that diffusion in the pipette is limiting the rate of diffusion from pipette to cell.

2. Time Constants, Electrode Shapes, and Electrode Resistance

From the computed values of the average intracellular concentrations at different times, we noticed that the

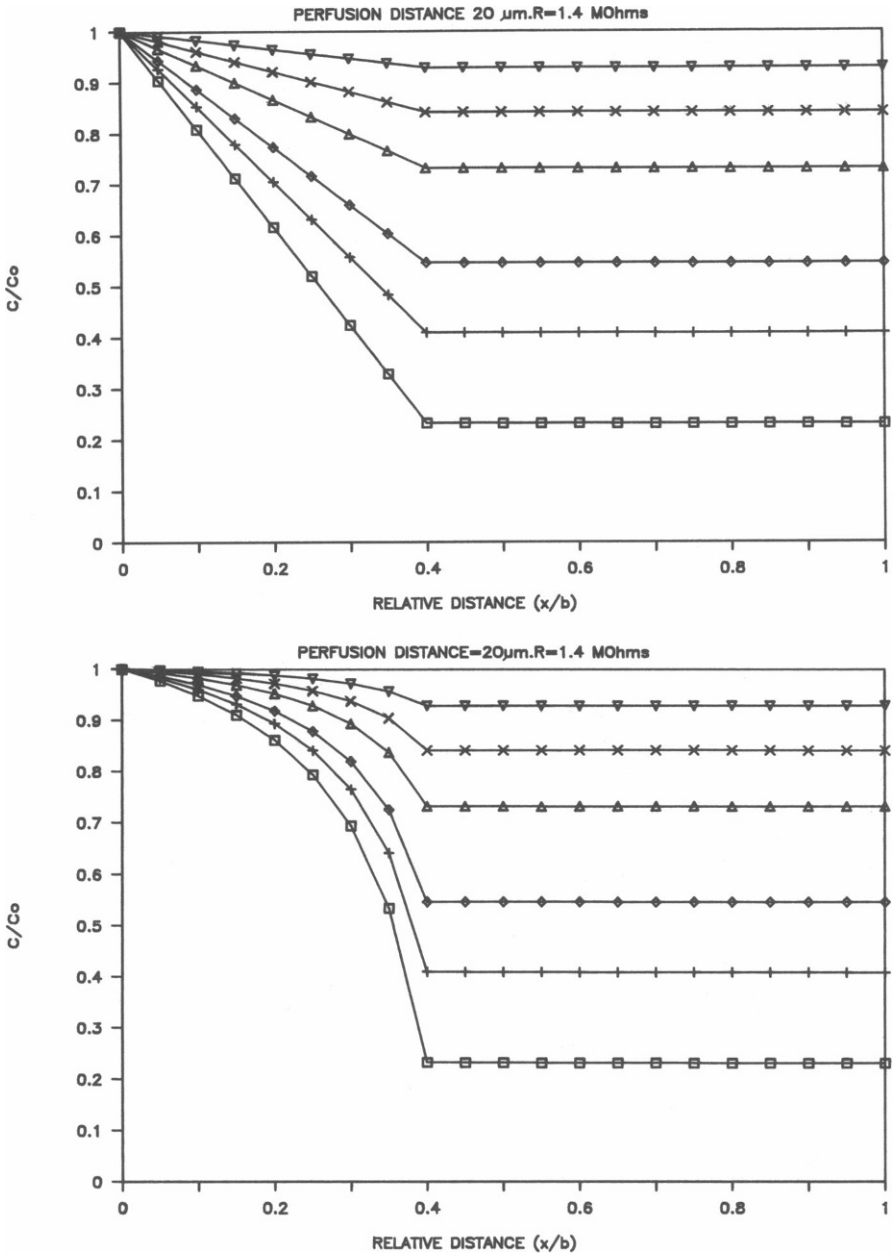

FIGURE 2 Concentration profiles in the pipette shank and cell at different times computed by numerically inverting the transformed concentrations derived in Appendix I. The upper figure shows the concentration profiles when the shank is cylindrical. The lower figure shows the concentration profiles when the shank is conical. The perfusion distance is 20 μm. The radius of the tip is 1 μm. The resistance of the shank between the perfusion point and the tip is 1.4 MΩ. The different symbols from bottom to top of each figure are the concentrations at 1, 2, 3, 5, 7, and 10 min from $t = 0$, respectively.

concentration vs. time values were well fitted by a single exponential. We calculated the time constants of these exponential transients by fitting a least squares straight line to the computed ln $(1 - \langle C(t)\rangle/Co)$ vs. t values. Where Co is the average intracellular concentration at steady state. There was always a good fit between the exponential and the $\langle C(t)\rangle$ values calculated numerically for at least 95% of the transient, see Fig. 3. The goodness of fit of the exponential transient to our calculations is indicated by the intercept of the least squares straight line of the ln $(1 - \langle C(t)\rangle/Co)$ vs. t values, which was always $<10^{-3}$. This implies that the exponential relaxation can be extrapolated to $t = 0$ to obtain the correct initial average intracellular concentration. The correlation coefficients were always >0.9999.

The pipette electrical resistance is an empirically determined parameter that depends on the tip size and shank geometry. Because these are the parameters that determine the time constant for diffusion, we examined the quantitative relationship between the electrical resistance of the electrode and the time constant to achieve steady state. We calculated the electrical resistance, R, between the perfusion point and the tip opening, as described in Appendix III. Fig. 4 shows numerical calculations of time constants to achieve steady state for cylindrical and conical shanks vs. their corresponding resistances. The time constants are directly proportional to the resistances. Moreover, a least squares regression line of time constants for conical shanks vs. time constants for cylindrical shanks, for pipette shanks having equal resistances, has a slope of 1.00,

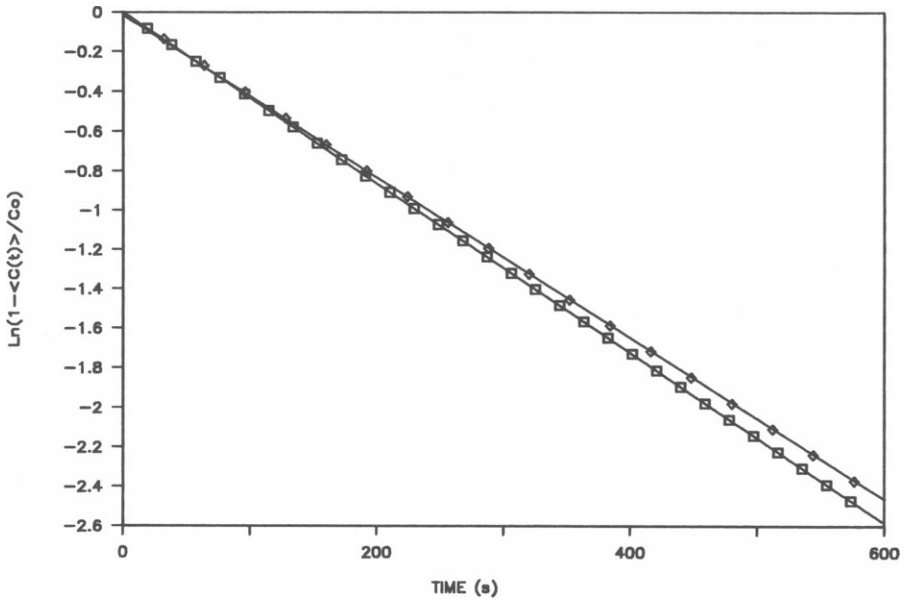

FIGURE 3 Time course of the spatially averaged intracellular concentration change computed by numerically inverting the average of the transformed intracellular concentration derived in Appendix I. The figure is a plot of $\ln(1 - \langle C(t)\rangle/Co)$ vs. t for a conical shank where $\langle C(t)\rangle$ is the average intracellular concentration at time t, and Co is the steady-state intracellular concentration. The radius of the tip is 1 μm, and its semi-cone angle is 12°. The squares and diamonds are the numerically calculated values for perfusion distances of 100 μm and infinite, respectively. The lines are the least squares straight lines for the respective numerical values.

intercept of −0.25 min, and correlation coefficient of 0.99 (graph not shown).

3. Numerical and Analytical TAUs

We also derived approximate analytic expressions for the late time constants to achieve steady state. We expanded the averaged Laplace transform of the intracellular concentration in a Taylor series and examined this expansion in the limit of very small s (see Appendix II). On the limit of small s, the expansion approached the Transform of an exponential function, and we extracted the time constant of this exponential. These late time constants for cylindrical and conical shanks are

$$\tau = \frac{A_c(b-a)a}{A_p D}; \tau = \frac{A_c(b-a)(d-a)a}{A_p D d},$$

where a, b, and d are the distances specified in Fig. 1. A_c and A_p are the cell and tip opening's cross-sectional areas, respectively. D is the diffusion coefficient of the diffusing particles. Fig. 5 shows a plot of numerical time constants vs. late time constants (calculated by using the analytic expressions shown above). From the figure, it is clear that the late time constants are good approximations to the time constants obtained numerically.

4. Effects of Perfusion Distance

We also derived an equation that expresses the late time constant as a function of R (see the details of the derivation in Appendix III).

$$\tau = \frac{VR}{D\rho},$$

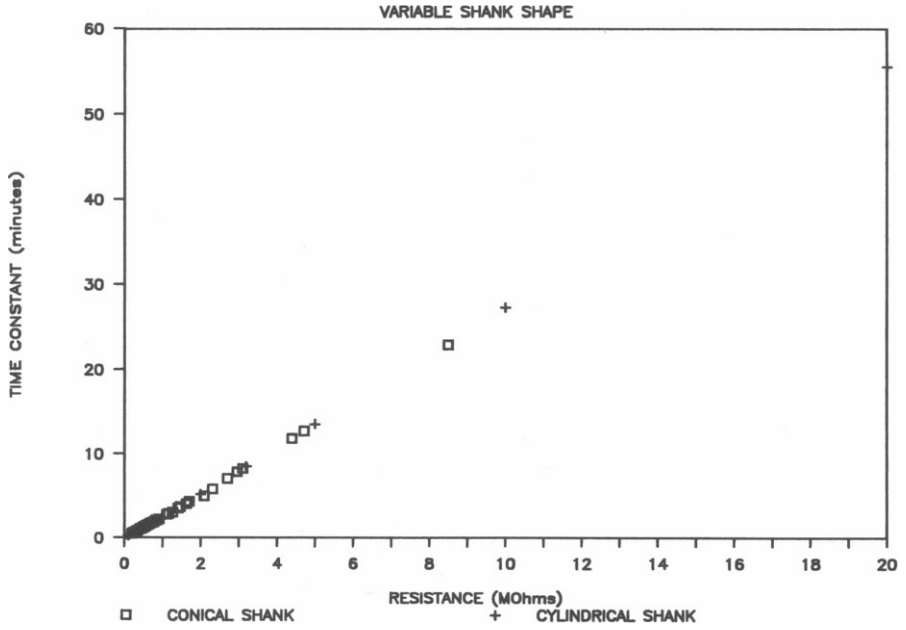

FIGURE 4 Time constants vs. shank resistances. The crosses are the numerically calculated time constants for cylindrical shanks. The squares are the time constants for conical shanks. In the calculations, we used perfusion distances and semi-cone angles that ranged between 10 and 150 μm and 5–40°, respectively. The electrode resistances were calculated as described in Appendix III.

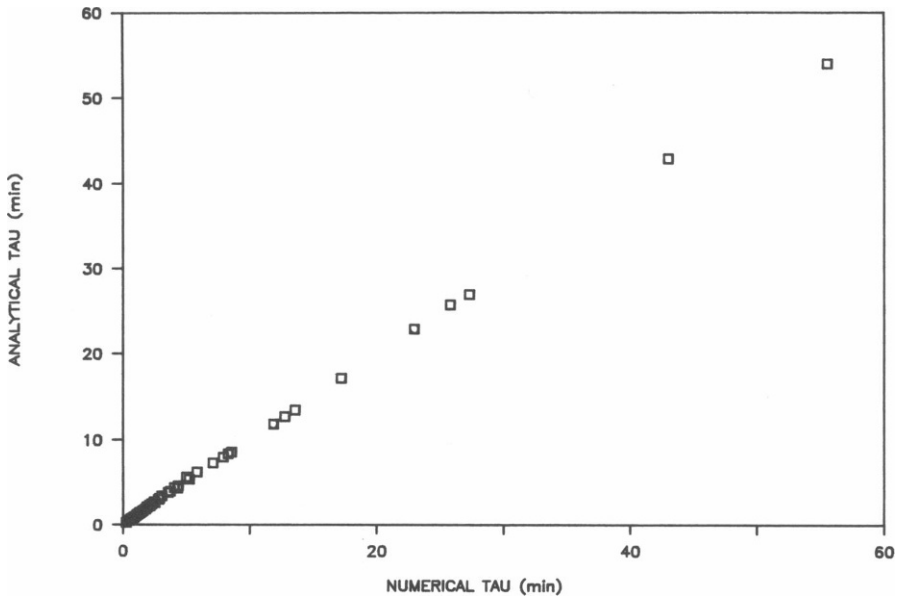

FIGURE 5 Numerical vs. analytic values of time constants. The figure shows a graph of the numerical vs. late time constants for the pipette shanks of Fig. 4. The slope of the least squares straight line for the values shown is 0.98, the intercept is 0.20, and the correlation coefficient is 0.98.

where V is the cell volume, R is the shank pipette resistance, and ρ is the resistivity of the pipette-filling solution.

If one examines the equation for the resistance of a conical pipette shank (see Appendix III, Eq. 1b), one notes that as the perfusion distance, a, increases the shank resistance approaches a limiting value. This occurs because the area of the base of a cone increases as the square of its height, so on increasing a, the increment in resistance approaches zero as $1/a$.

$$R = \frac{\rho}{\pi \tan(\alpha) r_p}.$$

For a tip opening radius of 1 μm and an angle of 12°, perfusion distances >20–50 μm are effectively infinite inasmuch as R attains its limiting value. Accordingly, the time constant calculated either analytically or numerically also tends to be independent of perfusion distance, and this is shown in Fig. 6. Moreover, for an infinite perfusion distance, the intracellular concentration still follows an exponential course with a time constant of 245.0 s (see Fig. 3). This time constant compares well with the time constant calculated from the limiting value of R (242.0 s).

The values of the pipette opening radius and α used above are not unrealistic for pipette electrodes routinely used in whole cell voltage clamping (8). The shank may assume a more cylindrical geometry near the tip, but, as described in the Discussion, it seems unlikely that this change in geometry will significantly alter our conclusions. Further, typical perfusion distances are on the order of hundreds of micrometers. One can conclude that for whole cell voltage clamp experiments, the time constant to

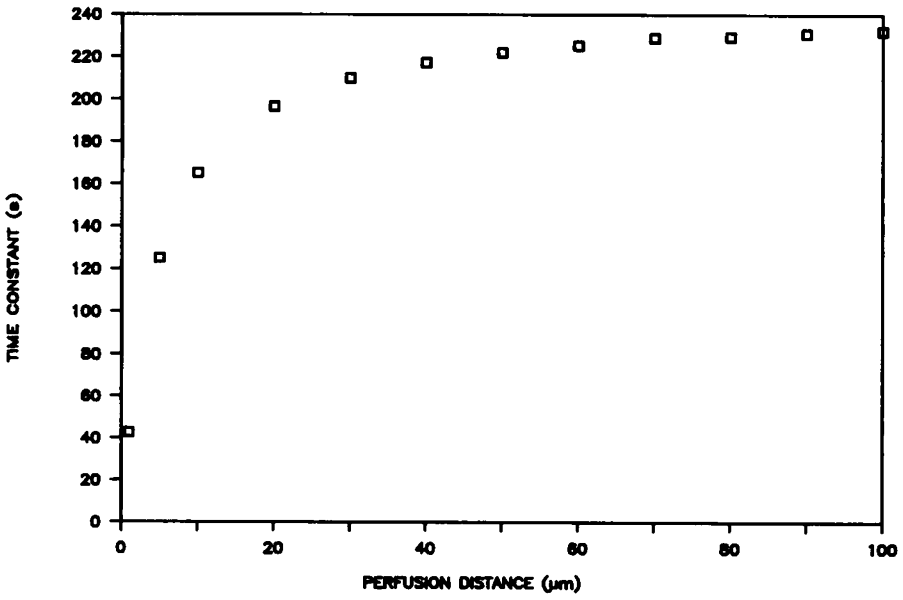

FIGURE 6 Time constant vs. perfusion distance. The figure is a plot of the numerical value of time constant vs. perfusion distance for a conical pipette shank. The semi-cone angle of the pipette is 12°. The tip radius is 1 μm.

achieve steady state and R could be estimated from the above limiting equations.

The calculations above suggest that, for practical purposes, the time constant to achieve steady state should be independent of whether the pipette is perfused or not. One might intuitively expect that the closer to the tip the perfusion the smaller the time constant to achieve steady state. However, from our model, it is evident that the perfusion distance has to be shorter than 20 μm for pipette perfusion to significantly reduce the time constant (see Fig. 6). The typical perfusion distance for an actual perfusion system is at least 100 μm, hence the time constant of perfused and unperfused pipettes will be similar.

5. Experimental and Analytical TAUs

Neher and Almers (9) studied the diffusion of Fura-2 from patch pipettes into Mast cells in the whole cell voltage clamp configuration. They measured the time constant to achieve steady state of intracellular fluorescence, for pipettes with different electrical resistances. They fitted a straight line to the experimental tau-electrode series resistance values. The least squares straight line they determined was

$$\tau = -6.44 + 5.965R_s(\text{M}\Omega).$$

We compared the experimentally determined slope of their equation with the slope we can calculate by using the expression for the late time constant to achieve steady state. We assumed that the total series resistance was equal to the shank pipette resistance plus other resistances in series with the shank resistance. The total electrode series resistance which we denote R_s is

$$R_s = R + R_p,$$

where R_p is the lumped resistance of all other resistances in series with R.

Under these assumptions, the equation for the time constant is

$$\tau = \frac{V}{D\rho}(R_s - R_p) = -\frac{VR_p}{D\rho} + \frac{V}{D\rho}R_s.$$

From Neher and Almers (9), we took the values for the cell volume and the diffusion constant of Fura-2. The diameter of the cells was 15 μm, and the diffusion constant of Fura-2 was $3 \cdot 10^{-6}$ cm^2/s. We assumed that the resistivity of the pipette-filling solution was 100 Ω-cm. The slope of the equation for the late time constant is 5.89 s/MΩ, and this value compares well with the slope of the least squares straight line found by Neher and Almers (5.965 s/MΩ). From the above equation and the data of Neher and Almers, R_p is roughly 1 MΩ.

Pusch and Neher (10) measured "normalized diffusion rates" for the exchange of 15 different substances between pipettes and bovine chromaffin cells in the whole cell patch clamp configuration. They followed the time course of the intracellular concentration as the substances were exchanged between the electrode and the intracellular space, and fitted exponentials to their data. The normalized diffusion rate they defined is the inverse of this time constant multiplied by the access resistance of the pipette-cell configuration. The access conductance was measured continuously during the course of the measurements.

We can obtain a theoretical expression from our model for the normalized diffusion rate. Assuming the access resistance is equal to R, the inverse late time constant multiplied by R should equal the normalized diffusion rate. From our theory, the normalized diffusion rate multiplied by the cell volume divided by the diffusion coefficient should equal the resistivity of the pipette filling solution. Pusch and Neher gave the diffusion coefficients of the substances they studied as well as the average volume of their cells. Using their data and our theory, the average value of the estimated resistivity of the pipette filling solution is 97 Ω-cm and the standard deviation is $\pm$55 Ω-cm. They employed pipettes filled with a 150 mM KCl solution, and the resistivity of such a solution is roughly 60 Ω-cm. This value is in reasonable agreement with the average extracted from Pusch and Neher's data (10). We ignored the rate constants for sodium and potassium in computing this average because they are severalfold faster than the theoretically expected values. We address the probable cause for the departure of sodium and potassium from the theoretical expectation in the Discussion, section 2.

DISCUSSION

1. External Forces

One of our assumptions is that no external forces act on the diffusing particles. If pressure gradients induce movement of the fluid in which the particles are dissolved, then an extra term should be added to the differential equation that describes the concentration of particles at a given point and time.

2. Membrane Transport

If the diffusing particles are transported out of the cell, then the steady-state intracellular concentration would be smaller than the one calculated by using our analysis. Substances normally present in cells may have membrane transporters, but substances not normally present in cells may not. Our model would be a more accurate representation of the diffusional process of this latter type of substance. From the results of Pusch and Neher (10), sodium and potassium achieve the steady state of intracellular concentration much faster than our model predicted, whereas the diffusion rates of the other substances they tested, which do not undergo transport or leak through the cell membrane, agreed well with our model. It is possible to show that if the transmembrane flux of the diffusing

particles varies proportionately to the intracellular concentration, the time to steady state would be decreased (work in progress).

3. Intracellular Binding

If the diffusing substance binds onto sites in the cell, changes in intracellular concentration could be significantly slowed. Similarly, if the diffusing substances are participants in a chemical reaction that occurs in the cell, the time necessary to achieve a steady state between the electrode and the cell would also be increased. This is equivalent to saying that the diffusing substances would disappear as they diffuse into the cell.

4. Minimum Time for Diffusion

Our model emphasizes the tip as the major barrier for the exchange of substances between the pipette and the cell. If other rate limiting barriers for intracellular diffusion are included in the modeling, then the calculated time to achieve the steady state of intracellular concentration could be significantly longer than the time one would calculate from our model.

5. Perfusion Distance

Our analysis suggests that the time constant to steady state is not significantly affected by perfusion, unless one can perfuse within some 20 μm from the pipette tip. This conclusion, as presented, is based on two observations: (*a*) the analytic expression for the time constant of a conical pipette, which is derived in Appendix II, is independent of perfusion distance, a, for values of 20 μm to 2 mm; (*b*) the numerical time constant for an unperfused conical pipette (i.e., a equals infinity) shows that the response is still a simple exponential with a time constant given by $VR/D\rho$. A thorough analytic treatment of the case when a tends to infinity is tedious and is therefore not presented. We did work through the analysis, however, and found that an infinite perfusion distance leads to a slow tail of concentration change, but the tail was several orders of magnitude too small to be observed. One can intuitively understand this result by visualizing the pipette geometry. The site of perfusion must be in a region where the pipette is significantly wider than its ~1 μm diameter tip, and in such a region, the volume of pipette solution is sufficiently large to maintain a nearly constant concentration, even if no perfusion is present. If the shank near the tip is more cylindrical in shape, it must widen at the site of perfusion. It is simple to calculate that even a 10 MΩ pipette, with a cylindrical shank geometry, must widen out to a more conical shape at a distance <10 μm from the tip. Thus, it seems unlikely that perfusion will be relevant to the time constant, regardless of the pipette shank geometry.

6. Diffusion Constant

As predicted by the analytic expression for the late time constant, the time constant to achieve steady state, calculated numerically, is inversely proportional to the diffusion constant of the diffusing particles (numerical calculations not shown). Therefore, particles with larger diffusion constants would have smaller time constants to achieve steady state.

CONCLUSIONS

From our modeling, we reached three main conclusions. First, the analytic expression we derived for the late time constant to achieve steady state agrees quantitatively well with our numerical computations. Hence, to approach the study of diffusion of substances from pipette to cell, in the framework of our model, one can use the analytic expression for the late time constant to estimate the time constant to achieve the steady state. Second, our analytic expression for the late time constant seems to be in good agreement with the time constant experimentally determined by Neher and Almers (9) and the data presented by Pusch and Neher (10). Further, Pusch and Neher concluded that pipette resistance, diffusion coefficient, and cell volume are the important experimental variables. Our theoretical analysis supports this experimental conclusion. This suggests that diffusion of substances from pipette to cell can be quantitatively described by our simple model. Third, our model predicts that the time constants to achieve steady state are the same whether the pipettes are perfused or not unless the perfusion distance is shorter than ~20 μm.

APPENDIX I

1. The differential equation that describes the diffusion of particles under the assumptions described in Theory and Methods is

$$\frac{\partial C(x,t)}{\partial t} = \frac{D}{A}\frac{\partial}{\partial x}\left[A\frac{\partial C(x,t)}{\partial x}\right]; 0 \le x \le b,$$

where x is the distance on the x axis from the origin of the coordinate axis (see Fig. 1). $C(x,t)$ is the concentration of the diffusing particles at distance x and time t. A is the area at distance x. D is the diffusion coefficient of the diffusing particles.

When the pipette shank is a cylinder, the area of the shank does not change with distance, and the diffusion equation is

$$\frac{\partial C(x,t)}{\partial t} = D\frac{\partial^2 C(x,t)}{\partial x^2}; 0 \le x \le a.$$

When the pipette shank is a cone, the diffusion equation is

$$\frac{\partial C(x,t)}{\partial t} = \frac{D}{\tan^2(\alpha)(d-x)^2}\frac{\partial}{\partial x} \cdot \left[\tan^2(\alpha)(d-x)^2\frac{\partial C(x,t)}{\partial t}\right]; 0 \le x \le a.$$

Initial conditions:

$$C(x,0) = C_0; 0 \le x \le a$$

$$C(x,0) = 0; a \le x \le b.$$

Boundary conditions:

$$C(0, t) = C_0; \text{ infinite source}$$

$$C(a^-, t) = C(a^+, t); \text{ continuity of concentration}$$

$$A_p \frac{\partial C(a^-, t)}{\partial x} = A_c \frac{\partial C(a^+, t)}{\partial x}; \text{ conservation of matter}$$

$$\frac{\partial C(b, t)}{\partial x} = 0; \text{ impermeable membrane.}$$

A_p is the area of the pipette tip. A_c is the cell cross sectional area. C_0 is the concentration of diffusing particles at the perfusion plane.

2. We define the Laplace transform of the concentration

$$\bar{C}(x, s) = \int_0^\infty C(x, t)e^{-st}\, dt.$$

The analytic expressions of the Laplace transformed concentrations are: (*a*) for a cylindrical shank,

$$\bar{C}(x, s) = \frac{C_0}{s} - \frac{C_0}{s} \cdot \frac{A_c \sinh\{g(b-a)\} \sinh\{gx\}}{\{A_p \cosh(ga) \cosh[g(b-a)] + A_c \sinh(ga) \sinh[g(b-a)]\}}; \quad 0 \le x \le a$$

$$\bar{C}(x, s) = \frac{C_0}{s} \cdot \frac{A_p \cosh\{ga\} \cosh\{g(b-x)\}}{\{A_p \cosh(ga) \cosh[g(b-a)] + A_c \sinh(ga) \sinh[g(b-a)]\}}; \quad a \le x \le b,$$

where $g^2 = s/D$.

(*b*) For a conical shank,

$$\bar{C}(x, s) = \frac{C_0}{s} - \frac{C_0 A_c g(d-a)^2 \sinh[g(b-a)] \sinh(gx)}{s(d-x)\{A_p \cosh[g(b-a)][g(d-a)\cosh(ga) + \sinh(ga)] + A_c g(d-a) \sinh[g(b-a)] \sinh(ga)\}}; \quad 0 \le x \le a$$

$$\bar{C}(x, s) = \frac{C_0 A_p [g(d-a)\cosh\{ga\} + \sinh\{ga\}] \cosh\{g(b-x)\}}{s\{A_p \cosh[g(b-a)][g(d-a)\cosh(ga) + \sinh(ga)] + A_c g(d-a) \sinh[g(b-a)] \sinh(ga)\}}; \quad a \le x \le b.$$

The average of the Laplace transformed intracellular concentration is defined as

$$\langle \bar{C}(s) \rangle = \frac{1}{(b-a)} \int_a^b \bar{C}(x, s)\, dx.$$

(*i*) When the shank is cylindrical,

$$\langle \bar{C}(s) \rangle = \frac{C_0}{sg(b-a)} \left\{ \frac{A_p \cosh(ga) \sinh[g(b-a)]}{A_p \cosh(ga) \cosh[g(b-a)] + A_c \sinh(ga) \sinh[g(b-a)]} \right\}$$

(*ii*) When the shank is conical,

$$\langle \bar{C}(s) \rangle = \frac{C_0}{sg(b-a)} \left\{ \frac{A_p[g(d-a)\cosh(ga) + \sinh(ga)] \sinh[g(b-a)]}{A_p \cosh[g(b-a)][g(d-a)\cosh(ga) + \sinh(ga)] + A_c g(d-a) \sinh[g(b-a)] \sinh(ga)} \right\}$$

APPENDIX II

(*a*) Cylindrical shank:

$$\langle \bar{C}(s) \rangle \simeq \frac{C_0}{s(1 + s\tau)}; \text{ when } s \text{ is small.}$$

$$\langle C(x, t) \rangle \simeq C_0[1 - e^{-t/\tau}],$$

where $\tau = \frac{A_c}{A_p} \frac{a(b-a)}{D} \left[1 + \frac{A_p}{A_c} \frac{b-a}{3a}\right]$.

For reasonable parameter values,

$$\tau \simeq \frac{A_c}{A_p} \frac{a(b-a)}{D}.$$

(*b*) Conical shank:

$$\langle \bar{C}(s) \rangle \simeq \frac{C_0}{s(1 + s\tau)}; \text{ when } s \text{ is small.}$$

$$\tau = \frac{A_c}{A_p} \frac{a(d-a)(b-a)}{Dd} \left\{1 + \frac{A_p}{A_c}\left[\frac{(b-a)d}{3(d-a)a} + \frac{a}{3(b-a)}\right]\right\}.$$

For reasonable parameter values and the perfusion distance, a, <2 mm,

$$\tau \approx \frac{A_c}{A_p} \frac{a(d-a)(b-a)}{Dd}.$$

APPENDIX III

(*a*) Pipette resistance

(*i*) Cylindrical shank:

$$R = \rho \frac{a}{\pi r_p^2}, \text{ where } r_p \text{ is the tip radius.}$$

(*ii*) Conical shank:

$$R = \frac{\rho}{\pi \tan(\alpha)} \left[\frac{1}{r_p} - \frac{1}{r_p + a \tan(\alpha)}\right].$$

(*b*) Relation between late time constant and R

(*i*) Cylindrical tip:

$$\tau = \frac{A_c}{A_p} \frac{a(b-a)}{D} = \frac{A_c(b-a)}{\pi r_p^2 D} a.$$

The cell volume is symbolized by V. Because $V = A_c(b-a)$, then from (*i*) above

$$\tau = \frac{V}{D} \frac{R}{\rho}.$$

(*ii*) Conical tip:

$$\tau = \frac{A_c}{A_p}\frac{a(d-a)(b-a)}{Dd} = \frac{A_c(b-a)}{D\pi r_p^2}\frac{a(d-a)}{d}.$$

Because $r_p(d-a) = \tan(\alpha)$,

$$\tau = \frac{V}{D}\frac{1}{\pi \tan(\alpha)}\left[\frac{1}{r_p} - \frac{1}{\tan(\alpha)d}\right].$$

Note that: $\tan(\alpha)d = \tan(\alpha)(d-a) + a\tan(\alpha) = r_p + a\tan(\alpha)$

$$\tau = \frac{V}{D}\frac{1}{\pi \tan(\alpha)}\left[\frac{1}{r_p} - \frac{1}{r_p + a\tan(\alpha)}\right]$$

$$\therefore \tau = \frac{V}{D}\frac{R}{\rho}.$$

This work was supported by National Institutes of Health grants EY06391, HL36075, HL20558, and PPG HL28958.

Received for publication 17 March 1988 and in final form 8 July 1988.

REFERENCES

1. Hamill, O. P., A. Marty, E. Neher, B. Sackmann, and F. Sigworth. 1981. Improved patch-clamp techniques for high-resolution current recording from cells and cell-free membrane patches. *Pfluegers Arch. Eur. J. Physiol.* 391:85–100.
2. Kameyama, M., F. Hoffmann, and W. Trautwein. 1985. On the mechanism of β-adrenergic regulation of the Ca^{+2} channel in the guinea-pig heart. *Pfluegers Arch. Eur.* 405:285–293.
3. Fischmeister, R., and H. C. Hartzell. 1986. Mechanism of action of acetylcholine on calcium current in single cells from frog ventricle. *J. Physiol. (Lond.).* 376:183–202.
4. Soejima, M., and A. Noma. 1984. Mode of Regulation of the ACh-sensitive K^+-channel by the muscarinic receptor in rabbit atrial cells. *Pfluegers Arch. Eur. J. Physiol.* 400:424–431.
5. Kimura, J., S. Miyamae, and A. Noma. 1987. Identification of sodium-calcium exchange current in single ventricular cells of guinea-pig. *J. Physiol. (Lond.).* 384:199–222.
6. Gadsby, D. C., J. Kimura, and A. Noma. 1985. Voltage dependence of Na^+/K^+ pump current in isolated heart cells. *Nature (Lond.).* 315:63–65.
7. Mogul, D., D. Singer, and R. TenEick. 1987. Intracellular diffusion of Na^+ from patch electrodes in cardiac myocytes: implications for Na^+ activity at internal Na^+ pump sites. *Biophys. J.* 51:261a. (Abstr.)
8. Sakmann, B., and E. Neher. 1983. Geometric parameters of pipettes and membrane patches. *In* Single-Channel Recording. B. Sakmann and E. Neher, editors. Plenum Publishing Corp., New York. 37–51.
9. Neher, E., and W. Almers. 1986. Patch pipettes used for loading small cells with fluorescent indicator dyes. *In* Biophysics of the Pancreatic β-Cell. I. Atwater, E. Rojas, and B. Soria. Plenum Publishing Corp., New York. 1–5.
10. Pusch, M., and E. Neher. 1988. Rates of diffusional exchange between small cells and a measuring patch pipette. *Pfluegers Arch. Eur. J. Physiol.* 411:204–211.